A Motorcyclist Anthropometric Test Device MATD

James A. Newman
Biokinetics and Associates Ltd.
Ottawa, Canada

John W. Zellner, Kenneth D. Wiley
Dynamic Research Inc.
Torrance, California

ABSTRACT

This paper reviews recent experience with a new test dummy intended principally for use in motorcycle crash testing.

MATD is a modified Hybrid III that contains an on-board data acquisition system and lower extremities that are capable of monitoring for leg and knee injuries. The femur and tibial complex are constructed of frangible elements whose biomechanical responses are based on available cadaver data. The knee is designed with fusible links that fail at load levels commensurate with that of human knee ligaments. The lower extremity assembly has been subjected to limited validation tests which are described.

The test device has been used in a series of full-scale car to motorcycle crash tests. The results of these tests provide new insight into the mechanisms of motorcycle crash-induced injuries. It also illustrates some limitations of MATD and suggests future development work to address some of these areas.

INTRODUCTION

In order to improve the crash-worthiness of motorcycles, crash testing analogous to that customarily employed in automobiles is becoming increasingly significant. However, the crash environment of the motorcyclist is very different from that of the automobile occupant. Anthropometric test devices (ATD's), which have been developed to assess automotive occupant crash safety are, as a consequence, not ideally suited as motorcyclist surrogates.

In 1989, St. Laurent et al [1] described the design and basic features of the first motorcyclist anthropometric test device, MATD 1. This crash test dummy is a pedestrian-style Hybrid III modified to be more suitable for motorcycle testing.

Among the modifications described is a 64-channel on-board data acquisition system. This feature completely eliminates the need for the customary electronic umbilical cord that, in the motorcycle crash environment, could significantly effect rider kinematics. This data acquisition system samples at 10,000 sec^{-1} per channel and is capable of recording up to 13 sec of the crash event. This is important since injuries can occur during the primary car to motorcycle crash as well as during subsequent rider contact with the ground. The complete listing for the 64-data channels (of which 50 were used) is given in the table in the Appendix.

The second significant modification was to the lower extremities of the dummy. The standard steel femur and tibias of the Hybrid III were replaced with frangible units whose strength and stiffness characteristics mimicked that of the human. In addition, the knee complex was redesigned to allow simulation of ligament rupture at the appropriate biomechanical levels.

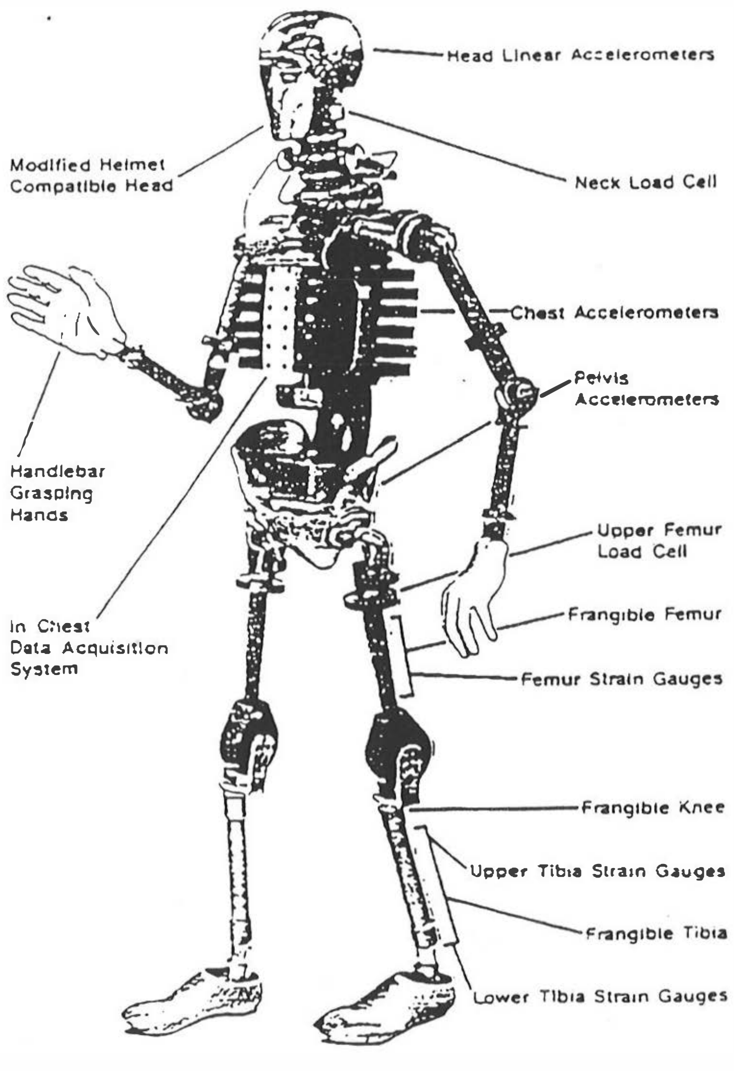

Figure 1: Motorcycle Dummy and Sensors

The purpose of these modifications was two-fold. Firstly, it provides a direct means to assess various significant lower extremity injuries. The design is such that the frangible elements monitor for fractures at all points on their length and circumference while the knee design provides direct evidence of the knee injury failure mechanisms. Secondly, it provides a more appropriate load path, and hence subsequent kinematics, in those cases when the crash would indeed be expected to produce a fracture or dislocation of a lower extremity.

In addition, 6 axis load cells were attached at the upper femurs and multi axis strain gauges were installed in the lower femurs and upper and lower tibias. These were used to verify the loads up to potential fracture and to allow analysis of time-dependence and cause-effect relationships. Additional refinements to the dummy included modifications to the head/neck region to facilitate helmet fitting and to the hands to facilitate gripping the motorcycle handle bars. Figure 1 is a schematic representation of MATD I.

DESIGN VERIFICATION

Knee Joint

The frangible knee assembly attaches directly to the base of the clevis of the existing Hybrid III knee, but it does not interfere with the knee in terms of flexion and extension. The design includes two brass pins which act as structural fuses, shearing when the load, in either torsion or varus-valgus rotation, exceeds the established tolerance levels. Appropriate response prior to failure is achieved by way of plastically deformable springs. Test results for the knee unit, in comparison to cadaver characteristics reported by St. Laurent [2], are provided in Figures 2 and 3. The surrogate knee response curves end at the points where their respective shear pins failed. As can be seen, the strength and stiffnesses are reasonably human-like for both forms of motion. The post-failure resistance to rotation is near zero for both modes.

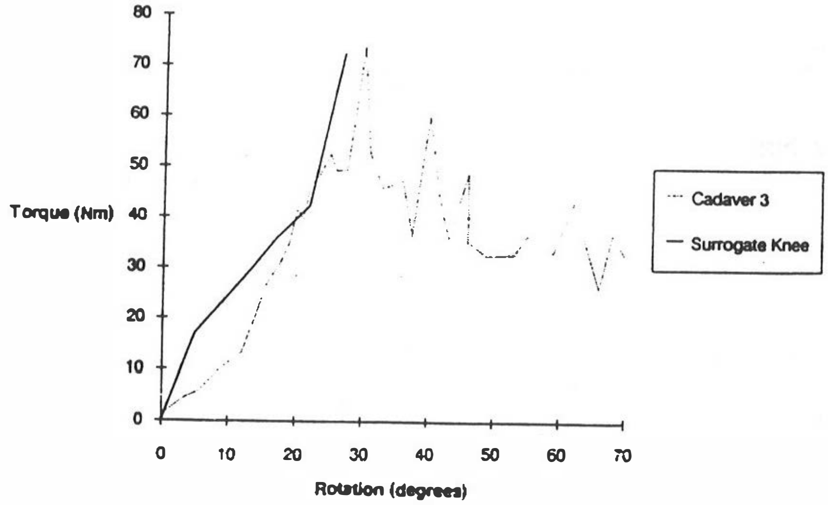

Figure 2: Response to Valgus Rotation of the Tibia [1]

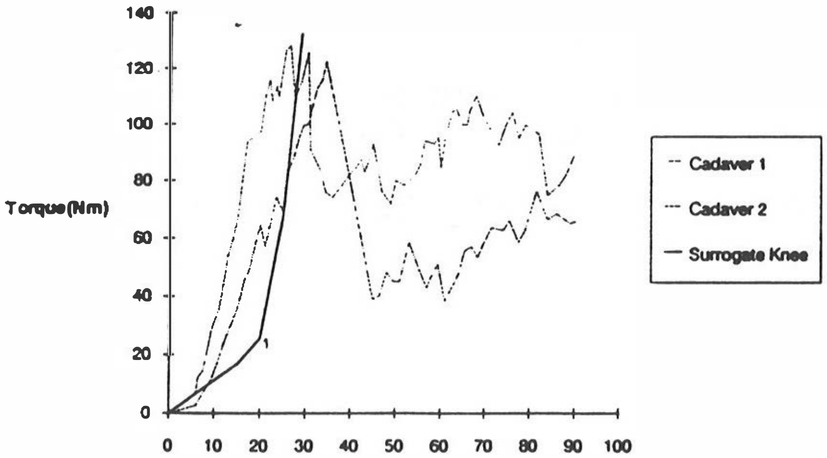

Figure 3: Response to External Torsional Rotation of the Tibia [1]

Leg Bones

Both the tibia and femur were constructed of composite materials. In essence, they are tubular in shape, wound with helical and axial glass fibres imbedded in a resin matrix. Bulkheads are used to prevent premature local tubular failure. Table 1 provides the results of a series of static tests in comparison with the design specifications.

Table 1: Design Verification, Static Tests

FEMUR

Static bending criteria 282.8 Nm

Test Data	Mean	Range	
285.8 Nm			
297.2 Nm	288.5 Nm	± 2.7%	(mean is 2% high)
282.6 Nm			

Static torsional criteria 165.7 Nm

Test Data	Mean	Range	
190.4 Nm			
177.7 Nm			
185.3 Nm	178.2 Nm	± 5.6%	(mean is 7% high)
172.9 Nm			
164.7 Nm			

TIBIA

Static bending criteria 253.3 Nm

Test Data	Mean	Range	
222.4 Nm			
239.0 Nm			
247.9 Nm			
275.1 Nm	241.4 Nm	± 6.4%	(mean is 5% low)
235.5 Nm			
239.9 Nm			
232.7 Nm			
238.6 Nm			

Static torsional criteria 117.0 Nm

Test Data	Mean	Range	
129.2 Nm			
134.4 Nm	127.2 Nm	± 10%	(mean is 8% high)
137.1 Nm			
108.3 Nm			

Figure 4 compares the tibial force deformation characteristics of the surrogate bone to data compiled by Yamada for simply supported static bending [3].

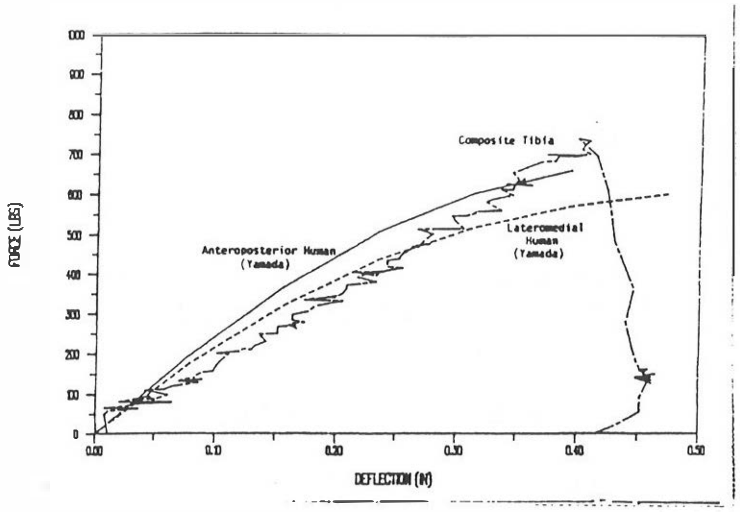

Figure 4: Tibia Force/Deflection Characteristics

In addition to static tests, the composite tibia has been subjected to impacts at the mid-span with a 76 mm diameter cylindrical anvil. These tests were meant to approximate the methods used by Fuller et al [4] in their dynamic tests of cadaver legs. Figure 5 compares the fracture response of the surrogate leg bone with the cadaver responses. The surrogate legbone lies within the force/time envelope of 9 cadavers and is somewhat stronger than 6 of the 9 cadavers. The time to fracture (less than 1 msec) verifies that the surrogate leg bone has an appropriate level of brittleness.

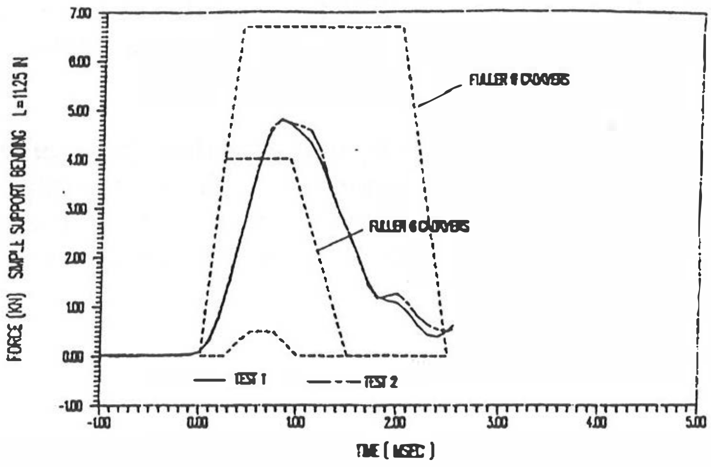

Figure 5: Composite Tibia Mid-Span Force vs Time
76 mm Dia Cylindrical Impactor Vel = 7.47 m/s

Leg Weights

The surrogate leg components were designed to have inertial properties very similar to those of a standard Hybrid III dummy. For example, the leg mass, including all components which articulate about the hip ball joint are, for the Hybrid III; 14.8 kg, for the MATD; 15.1 kg.

FULL-SCALE CRASH TESTING

Analysis of Crash Test Results

MATD I has been used in 16 full-scale car vs motorcycle impact tests. The details of these tests have been described in [5]. During these tests the dummy was subjected to some extraordinarily violent collisions.

Following each test, the dummy data was analyzed to determine:

a) number and causation of leg bone and knee ligament failures
b) head trajectory and velocity
c) head maximum resultant acceleration[1]
d) overall predicted injury severity and injury costs

The latter measure provided a common basis of comparison of tests which resulted in different types and severity of predicted injuries. To illustrate the analysis of predicted leg injury cause and effect, a typical example follows.

> Post-test inspection of the dummy revealed a broken left femur frangible element. The data from the left femur load cell showed a sustained steady compression load F_z, high M_x and M_y moments and a discontinuity at t = .072 sec. Review of the objective data from the left femur frangible element strain gauges shows loss of signal (gauge failure) at t = .072 sec. Review of high speed film shows that at t = .072 sec. the dummy hips are moving forward and the left knee is in contact with a proposed energy absorbing device designed to limit compression loads
>
> The steady femur compression force F_z indicates that the energy absorbing device did limit the femur compression force, however, relative motion between the dummy hips, the fixed knee and lateral leg restraint produced substantial fore/aft and lateral bending moments, causing fracture of the femur.

[1] In these tests, rotational acceleration of the head was not measured and head injury severity (and its cost) was related only to the maximum resultant translational acceleration.

SUMMARY

A new test dummy, intended principally for use in motorcycle crash testing, has been developed and used in recent full-scale tests. Innovative features include a 64 channel on-board data acquisition system, and frangible femur, tibia and knee ligament components.

Validation tests to date show that the stiffness and fracture properties of the surrogate leg components match the properties of cadaver subjects in static and limited dynamic tests.

Experience in full-scale crash tests shows the MATD to be a practical and effective tool for determining detailed cause-effect relationships pertinent to motorcyclist leg fracture phenomena. Its effectiveness comes at some cost in complexity of use. However, after an initial learning period, dummy cycling time was reduced to under 4 hours with a crew of 4 highly-trained individuals. This included the time required to download data to host computers, replace the frangible hardware, check the function of the 50 data channels, reassemble the dummy components, dress the dummy with helmet, coveralls and boots, and install the dummy on the motorcycle ready for the next test.

Overall, the MATD prototype performed quite well. A major reason for this is the inherently rugged design of the Hybrid III and of the specially designed data acquisition system. Loss of data due to sensor failures, data acquisition problems and broken conductors was about 5% of the total test/channel combinations.

One limitation of this first MATD was an inappropriate thorax compliance. This was associated with the packaging of the data acquisition system which limited the degree to which thoracic injuries could be monitored. In the future, further down-sizing of the on-board electronics will allow for more chest deformation and the ability to better monitor for thoracic injury.

REFERENCES

1. St. Laurent, A., Szabo, T., Shewchenko, N. and Newman, J.A., "Design of a Motorcyclist Anthropometric Test Device". 12th International Technical Conference on Experimental Safety Vehicles, Goteborg, Sweden, 1989.

2. St. Laurent, A., Shewchenko, N., Szabo, T., "Development of Frangible Knee and Hip Elements for a Motorcycle ATD (Summary)". Document R89-4 to Dynamic Research, Inc., Torrance, California, January, 1989.

3. Yamada, H., "Strength of Biological Materials". Edited by F.G. Evans, Williams and Wilkins, 970.

4. Fuller, P.M., Snider, J.N., "Dynamic Response of the Human Leg to Impact Loading, Third Year Report, Research Overview 1986-1989, Volume 1". Department of Anatomy, School of Medicine, University of Louisville, Louisville, KY and Industrial Engineering Department, University of Tennessee, Knoxville, TN, April, 1989.

5. Sakamoto, S., "Research History of Motorcycle Leg Protection". SAE Paper No. 900755, presented at the International Congress and Exposition, Detroit, MI, 1990.

Appendix: List of Sensors

Channel	Location	Measure	Sensor
1	Head	a_x	Endevco 7231C
2	Head	a_y	Endevco 7231C
3	Head	a_z	Endevco 7231C
4	Pelvis	a_x	Endevco 7231C
5	Pelvis	a_y	Endevco 7231C
7	Spare		
8	Spare		
9	Right Upper Femur	F_x	Denton 2181
10	Right Upper Femur	F_y	Denton 2181
11	Right Upper Femur	F_x	Denton 2181
12	Right Upper Femur	M_x	Denton 2181
13	Right Upper Femur	M_y	Denton 2181
14	Right Upper Femur	M_z	Denton 2181
15	Spare		
16	Spare		
17	Neck	F_x	Denton 1716
18	Neck	F_y	Denton 1716
19	Neck	F_z	Denton 1716
20	Neck	M_x	Denton 1716
21	Neck	M_y	Denton 1716
22	Neck	M_z	Denton 1716
23	Spare		
24	Spare		
25	Chest	a_x	Endevco 7231C
26	Chest	a_y	Endevco 7231C
27	Chest	a_z	Endevco 7231C
28	Head	a_x	Endevco 7231C
29	Head	a_y	Endevoc 7231C
30	Head	a_z	Endevco 7231C
31	Spare		
32	Spare		
33	Left Lower Tibia	Pz_1	Axial Strain Gauge
34	Left Lower Tibia	Pz_2	Axial Strain Gauge
35	Left Lower Tibia	M_x	2 Axial Strain Gauges
36	Right Lower Tibia	Pz_1	Axial Strain Gauge
37	Right Lower Tibia	Pz_2	Axial Strain Gauge
38	Right Lower Tibia	M_x	2 Axial Strain Gauges
39	Spare		
40	Spare		
41	Left Upper Femur	F_x	Denton 2181
42	Left Upper Femur	F_y	Denton 2181
43	Left Upper Femur	F_z	Denton 2181
44	Left Upper Femur	M_x	Denton 2181

Channel	Location	Measure	Sensor
45	Left Upper Femur	M_y	Denton 2181
46	Left Upper Femur	M_z	Denton 2181
47	Spare		
48	Spare		
49	Right Upper Tibia	M_x	2 Axial Strain Gauges
50	Right Upper Tibia	M_y	2 Axial Strain Gauges
51	Right Upper Tibia	M_z	Shear Strain Gauge
52	Left Upper Tibia	M_x	2 Axial Strain Gauges
53	Left Upper Tibia	M_y	2 Axial Strain Gauges
54	Left Upper Tibia	M_z	Shear Strain Gauge
55	Spare		
56	Spare		
57	Left Frangible Femur	Pz_1	Axial Strain Gauge
58	Left Frangible Femur	Pz_2	Axial Strain Gauge
59	Left Frangible Femur	M_x	2 Axial Strain Gauges
60	Left Frangible Femur	M_z	Shear Strain Gauge
61	Right Frangible Femur	Pz_1	Axial Strain Gauge
62	Right Frangible Femur	Pz_2	Axial Strain Gauge
63	Right Frangible Femur	M_x	2 Axial Strain Gauges
64	Right Frangible Femur	M_z	Shear Strain Gauge